Updated Constraints and Forecasts on Primordial Tensor Modes

Giovanni Cabass

Physics Department and INFN, Università di Roma "La Sapienza"

In collaboration with:

L. Pagano, L. Salvati, M. Gerbino, E. Giusarma, A. Melchiorri (arXiv: 1511.05146)

Outline

- Introduction
- Primordial gravitational waves – observable effects
  - CMB B-mode polarization
  - contribution to radiation energy density
- Constraints on primordial tensor spectrum, with and without BK14 data
- Forecasts
  - COrE-like mission
  - COrE + AdvLIGO

Introduction

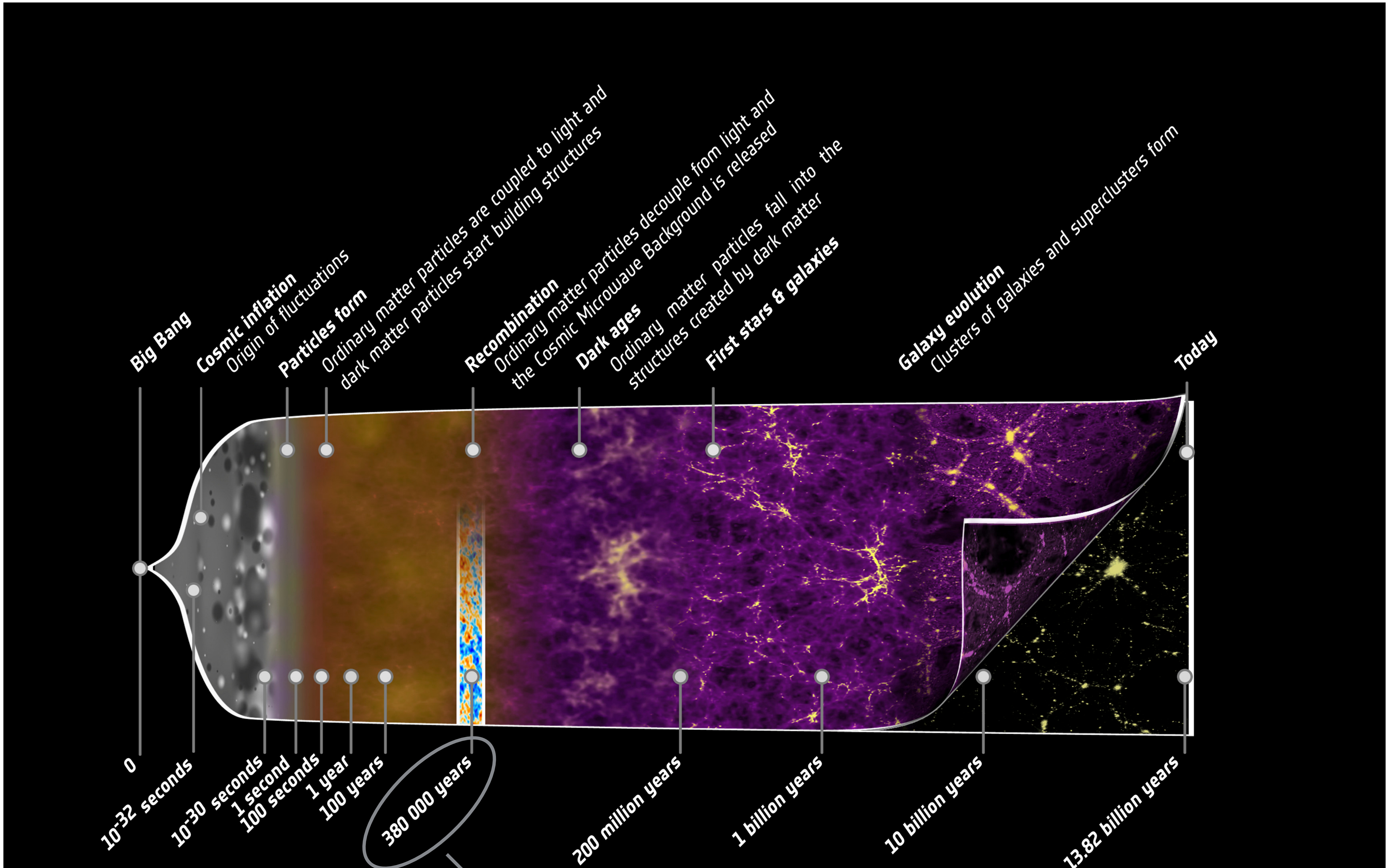

CMB decoupling: $z \simeq 1100$, $T \simeq 2.7(1+z)$ K

CMB as probe of primordial perturbations

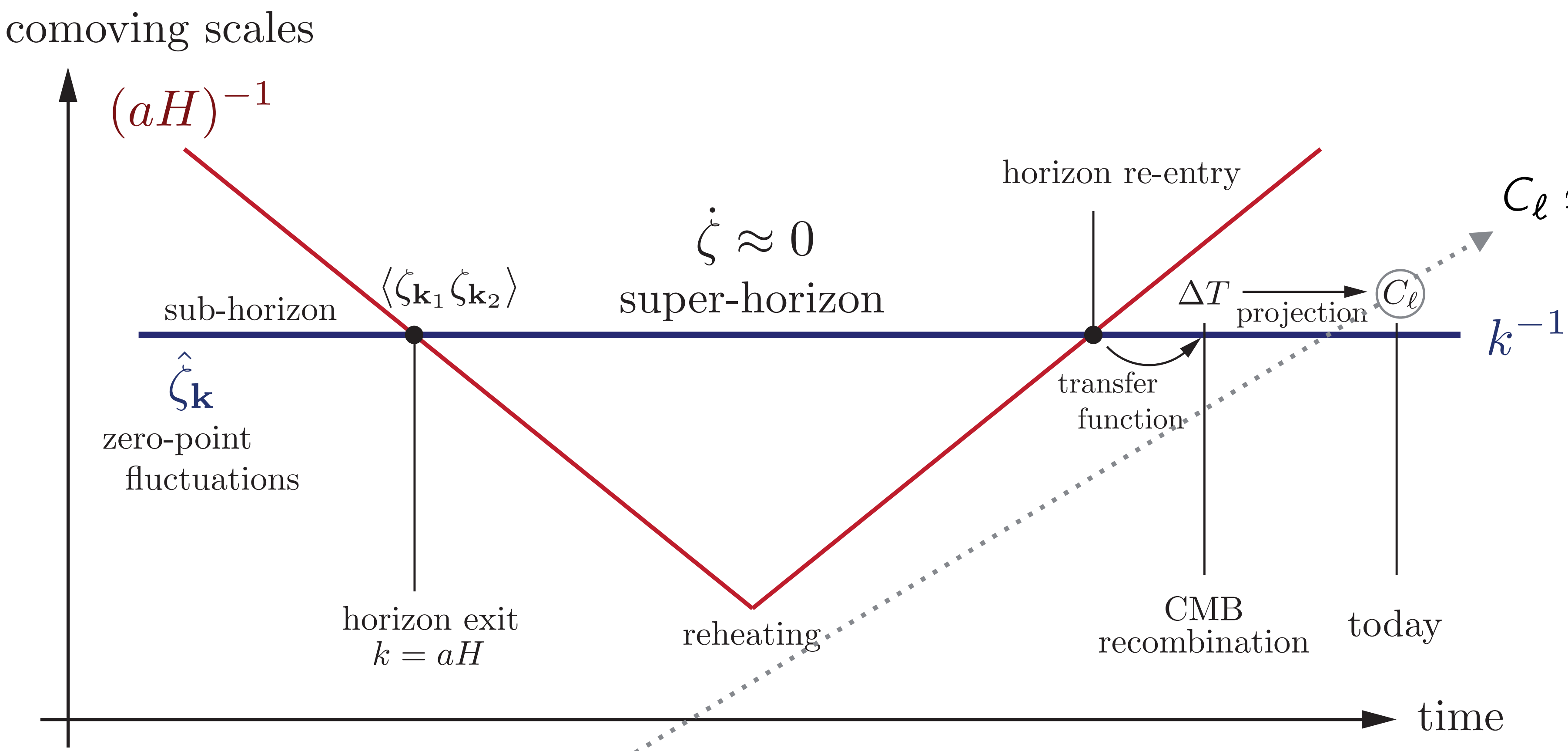

Baumann, 2009

$$C_\ell \simeq \left\langle \frac{\delta T}{T}(\theta) \frac{\delta T}{T}(\theta') \right\rangle \longleftrightarrow P_\zeta(k)$$

$$\frac{k^3}{2\pi^2} P_\zeta(k) = A_s \left(\frac{k}{k_\star} \right)^{n_s - 1}$$

with $n_s = \underbrace{0.9645}_{} \pm 0.0049$

almost flat (red) spectrum

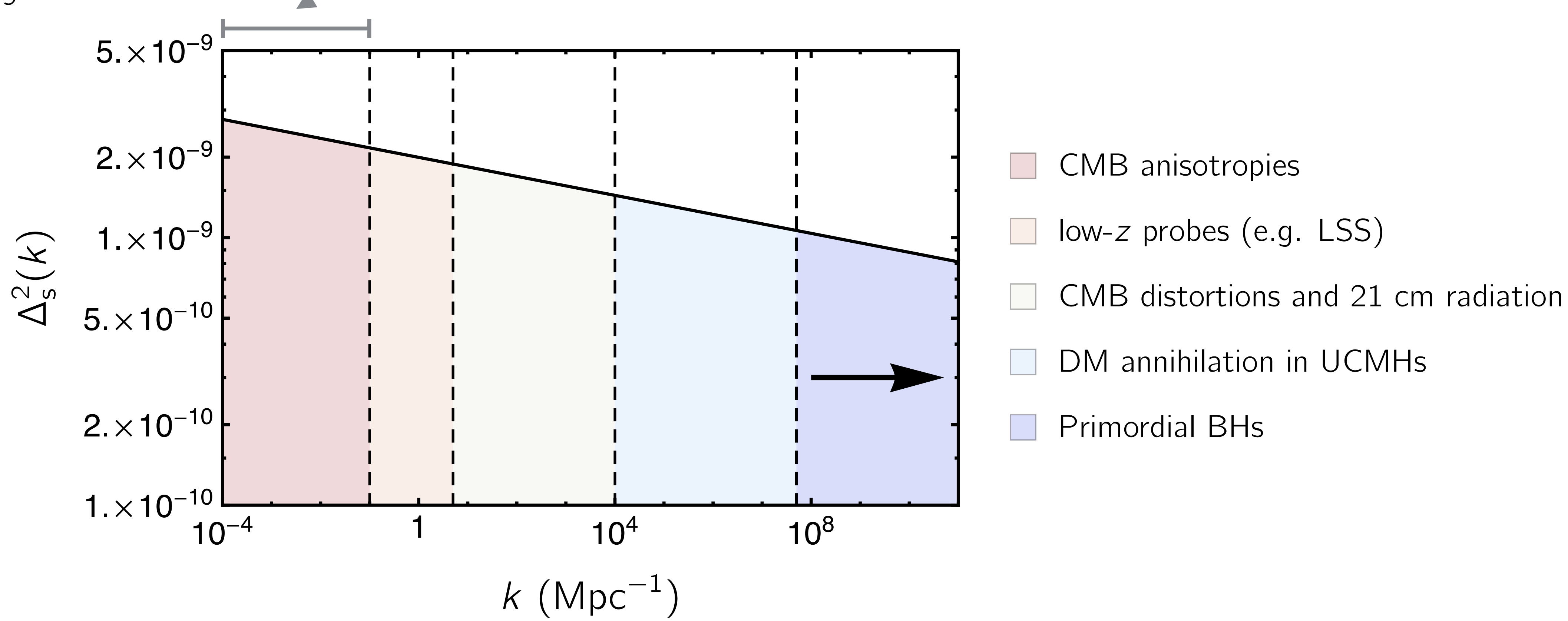

Observable Signatures of Primordial Tensor Modes

CMB polarization

We expect the CMB to become polarized via Thomson scattering: $\frac{d\sigma}{d\Omega} \propto |\hat{\boldsymbol{\epsilon}} \cdot \hat{\boldsymbol{\epsilon}}'|$

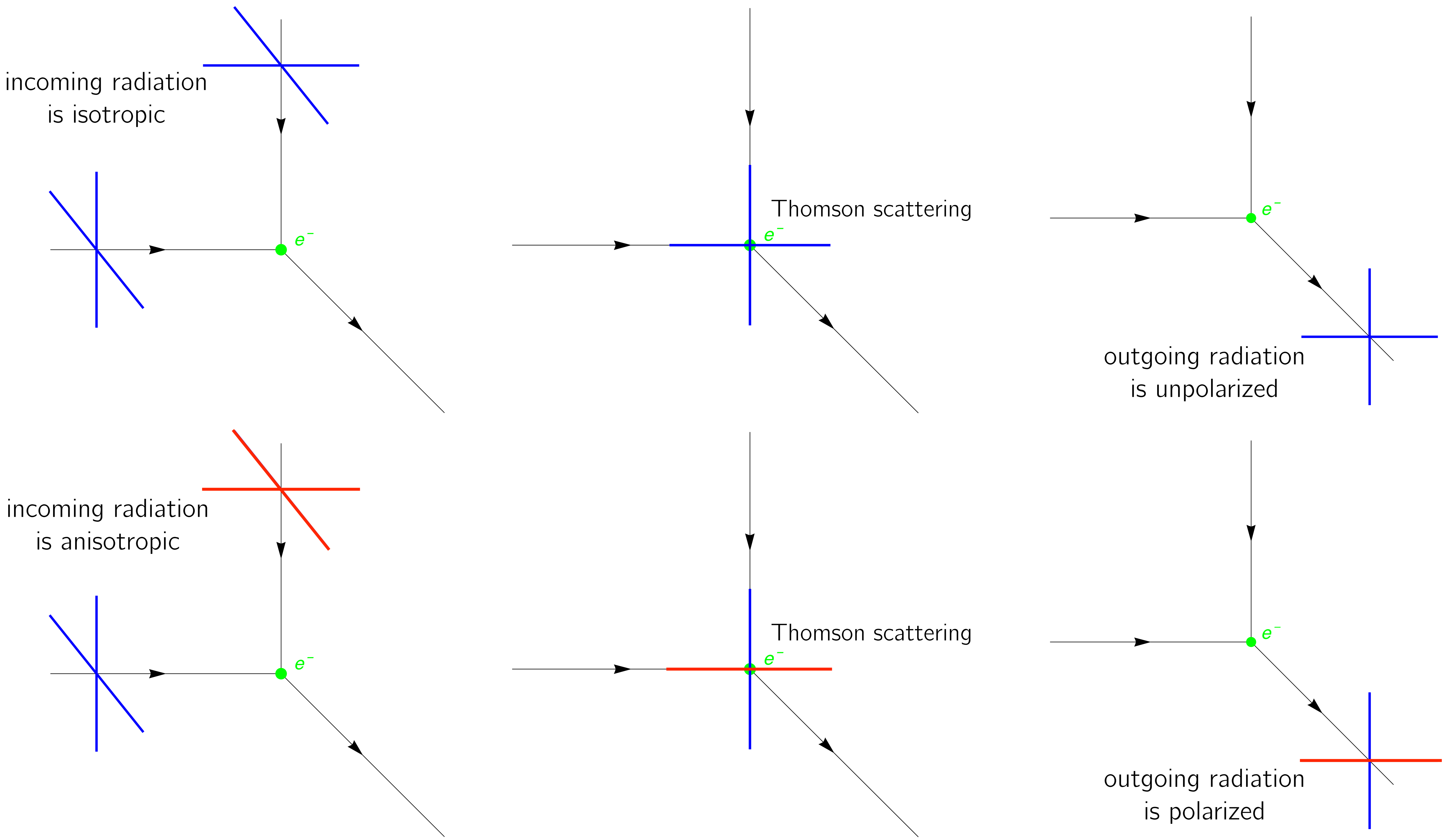

E- and B-mode polarization pattern

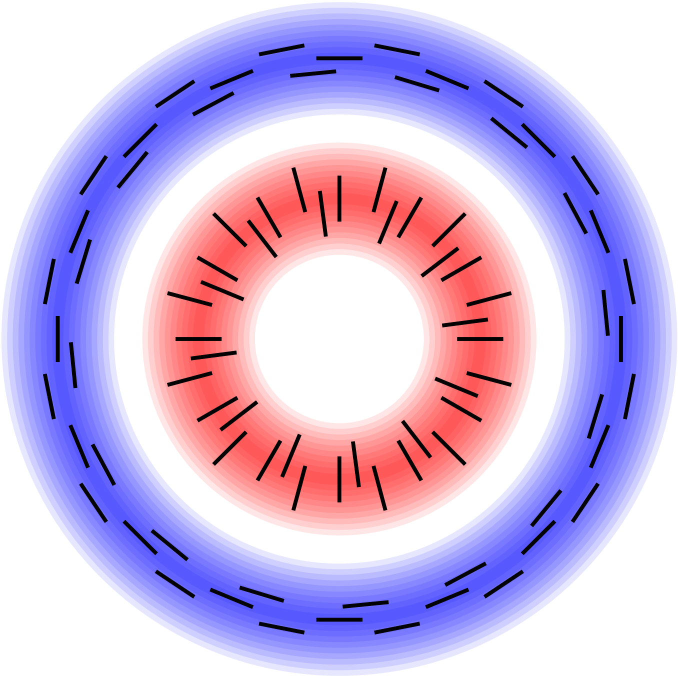

E-mode polarization around cold spot

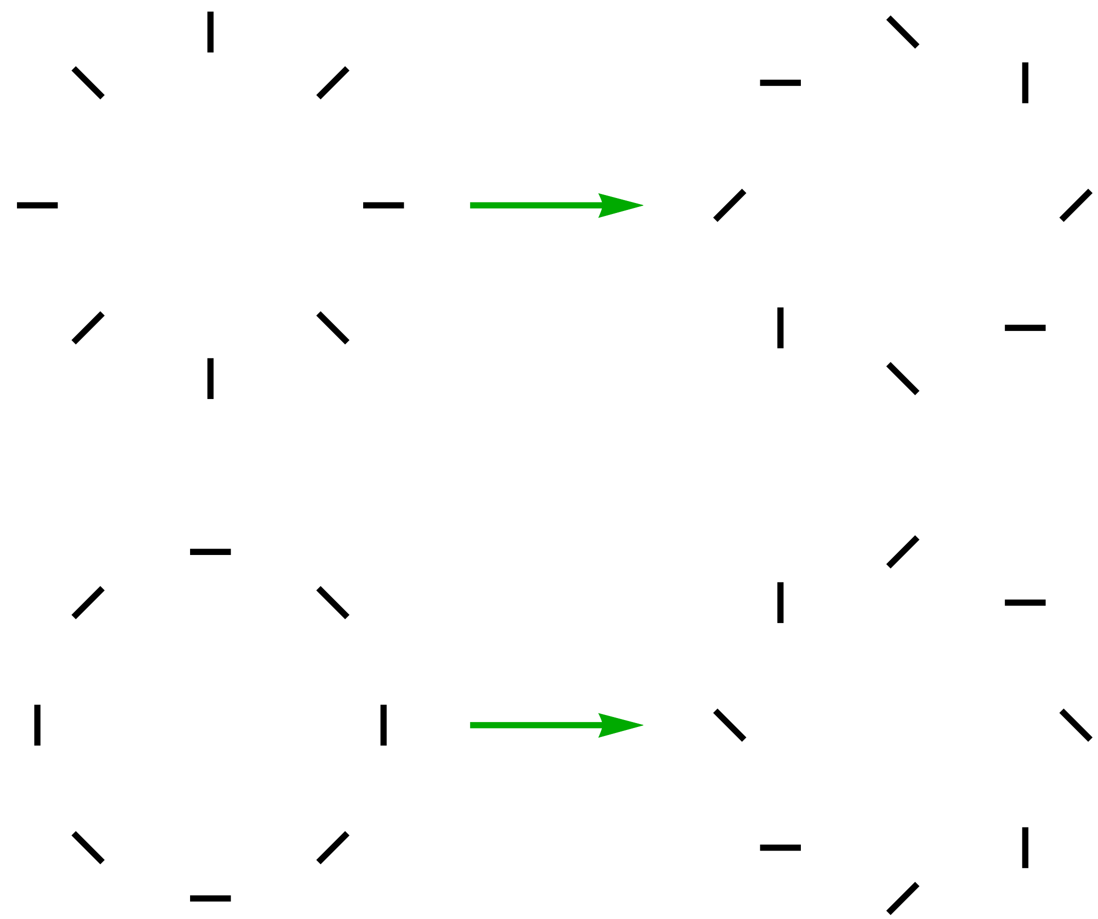

from E-mode to B-mode polarization

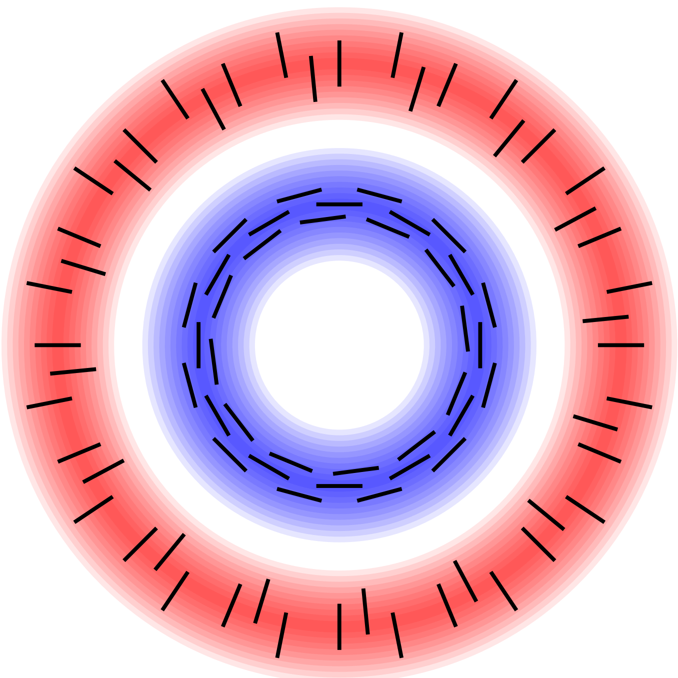

E-mode polarization around hot spot

- E-mode pattern: invariant for $\hat{\boldsymbol{n}} \to -\hat{\boldsymbol{n}}$;
- B-mode pattern: odd under $\hat{\boldsymbol{n}} \to -\hat{\boldsymbol{n}}$.

Tensor perturbations and B-modes

Quantum fluctuations of spatial metric h_{ij} $\to$ two-point function $P_{\rm t}(k)$:

$$h_{ij}(x) = \int \frac{\mathrm{d}\boldsymbol{k}}{(2\pi)^{3/2}} \sum_{p=+,\times} \epsilon^p_{ij}(\boldsymbol{k}) h^p_{\boldsymbol{k}}(t) e^{i\boldsymbol{k}\cdot\boldsymbol{x}} \longrightarrow \langle h^p_{\boldsymbol{k}} h^q_{\boldsymbol{k}'}\rangle' = P_{\rm t}(k)$$

Need quadrupole anisotropy to polarize CMB photons. Both scalar and tensor modes source a quadrupole anisotropy $\to$

$$C^{XY}_\ell = \int \mathrm{d}\log k\, \Delta^X_{\mathrm{s},\ell}(k)\Delta^Y_{\mathrm{s},\ell}(k) P_{\rm s}(k) + \int \mathrm{d}\log k\, \Delta^X_{\mathrm{t},\ell}(k)\Delta^Y_{\mathrm{t},\ell}(k) P_{\rm t}(k)$$

- tensor perturbations $h^p_{\boldsymbol{k}}$ generate both E-modes and no B-modes.
- scalar perturbations $\zeta_{\boldsymbol{k}}$ generate E-modes, but no B-modes: transfer functions $\Delta^B_{\mathrm{s},\ell}$ are 0;

⇨ angular power spectra of B-mode polarization C^{BB}_ℓ allow to probe the primordial tensor spectrum

GW contribution to radiation energy density

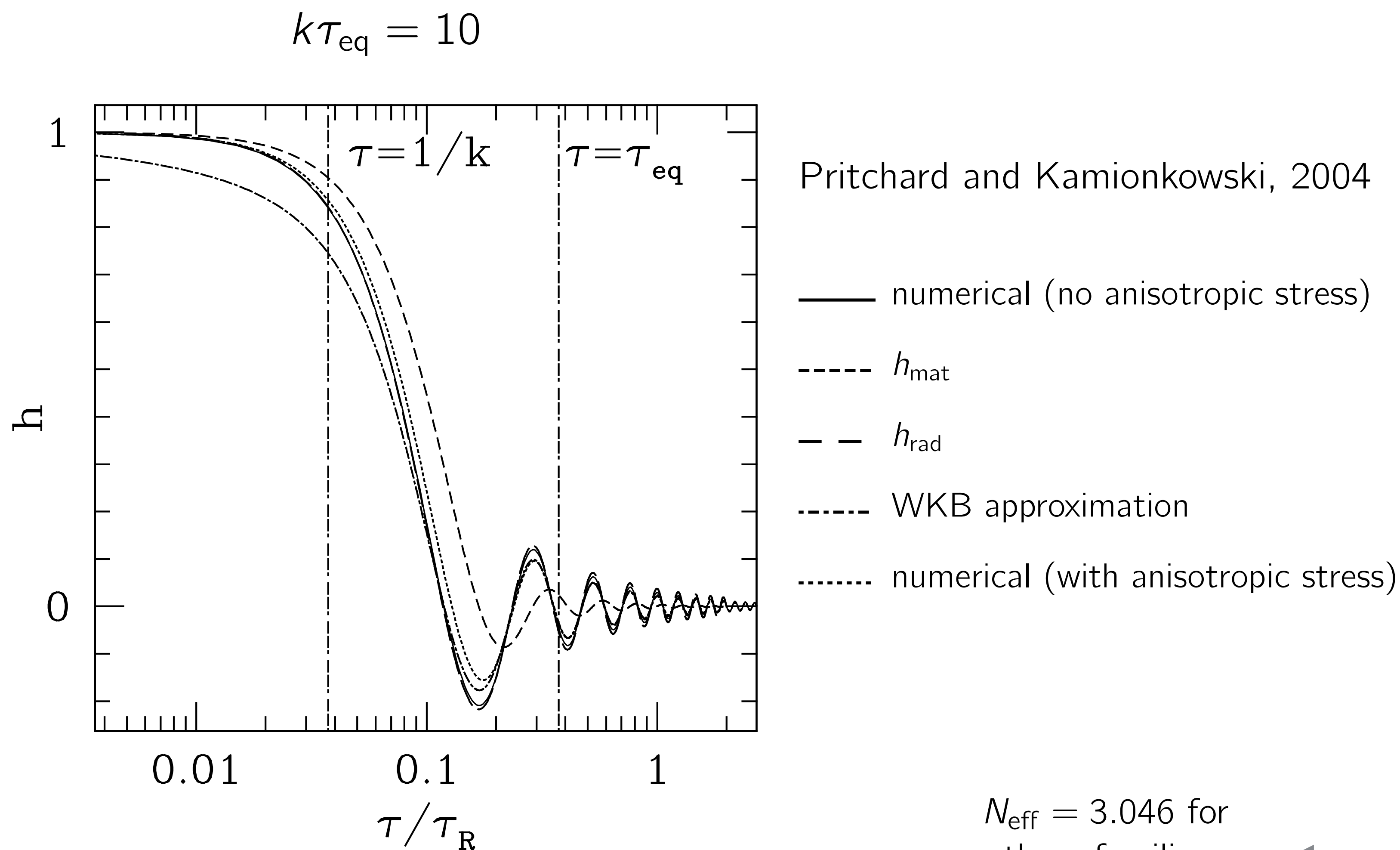

Pritchard and Kamionkowski, 2004

tensor modes re-enter the horizon
→ they begin to oscillate

⇩

propagate as massless modes
→ contribute to $\rho_{\rm rad}$

⇩

$$\Omega_{\rm rad} = \Omega_\gamma \left[1 + \frac{7}{8}\left(\frac{4}{11}\right)^{\frac{4}{3}} N_{\rm eff}\right]$$

← $N_{\rm eff} = 3.046$ for three families of neutrinos

Maggiore, 1999

$$N_{\rm eff}^{\rm GW} = \frac{h_0^2}{5.6\times 10^{-6}}\int_{f_{IR}}^{f_{UV}} {\rm d}\log f\,\Omega_{\rm GW}(f)$$

with

$$\Omega_{\rm GW}(f) = \frac{1}{\rho_c}\frac{\rho_{\rm GW}}{{\rm d}\log f}$$

IR and UV cutoffs, primordial tensor spectrum

The integral for $N_{\rm eff}^{\rm GW}$ does not extend on all frequencies:

- at a given redshift, there is a IR cutoff equal to the horizon size at that redshift. Energy of superhorizon modes is zero (they are frozen out);
- the UV cutoff is more arbitrary. In our analysis we take f_{UV} to be the horizon size at the end of inflation ($k_{UV} \approx 2 \times 10^{23}\,{\rm Mpc}^{-1}$).

$$\Omega_{\rm GW}(f) = \frac{\Delta_{\rm t}^2(f)}{24 z_{\rm eq}}, \text{ with } f/{\rm Hz} = 1.6 \times 10^{-15} k/{\rm Mpc}^{-1}$$

Ungarelli et al., 2005
Watanabe and Komatsu, 2006

$$\text{for } \Delta_{\rm t}^2(k) = r A_{\rm s} \left(\frac{k}{k_\star}\right)^{n_{\rm t}} \Rightarrow N_{\rm eff}^{\rm GW} \approx 3 \times 10^{-6} \times \frac{r A_{\rm s}}{n_{\rm t}} \left[\left(\frac{f}{f_\star}\right)^{n_{\rm t}}\right]_{f_{IR}}^{f_{UV}}$$

Constraints at different frequencies

(see also Meerburg et al., 2015)

- $N_{\rm eff}^{\rm BBN}$: contribution of GWs to $\rho_{\rm rad}$ at BBN. A large $N_{\rm eff}^{\rm BBN}$ will result in an overproduction of ^{4}He. The IR cutoff is the horizon size at BBN;
- $N_{\rm eff}^{\rm CMB}$: contribution of GWs to $\rho_{\rm rad}$ at decoupling. It affects CMB anisotropies. The IR cutoff is the horizon size at decoupling.

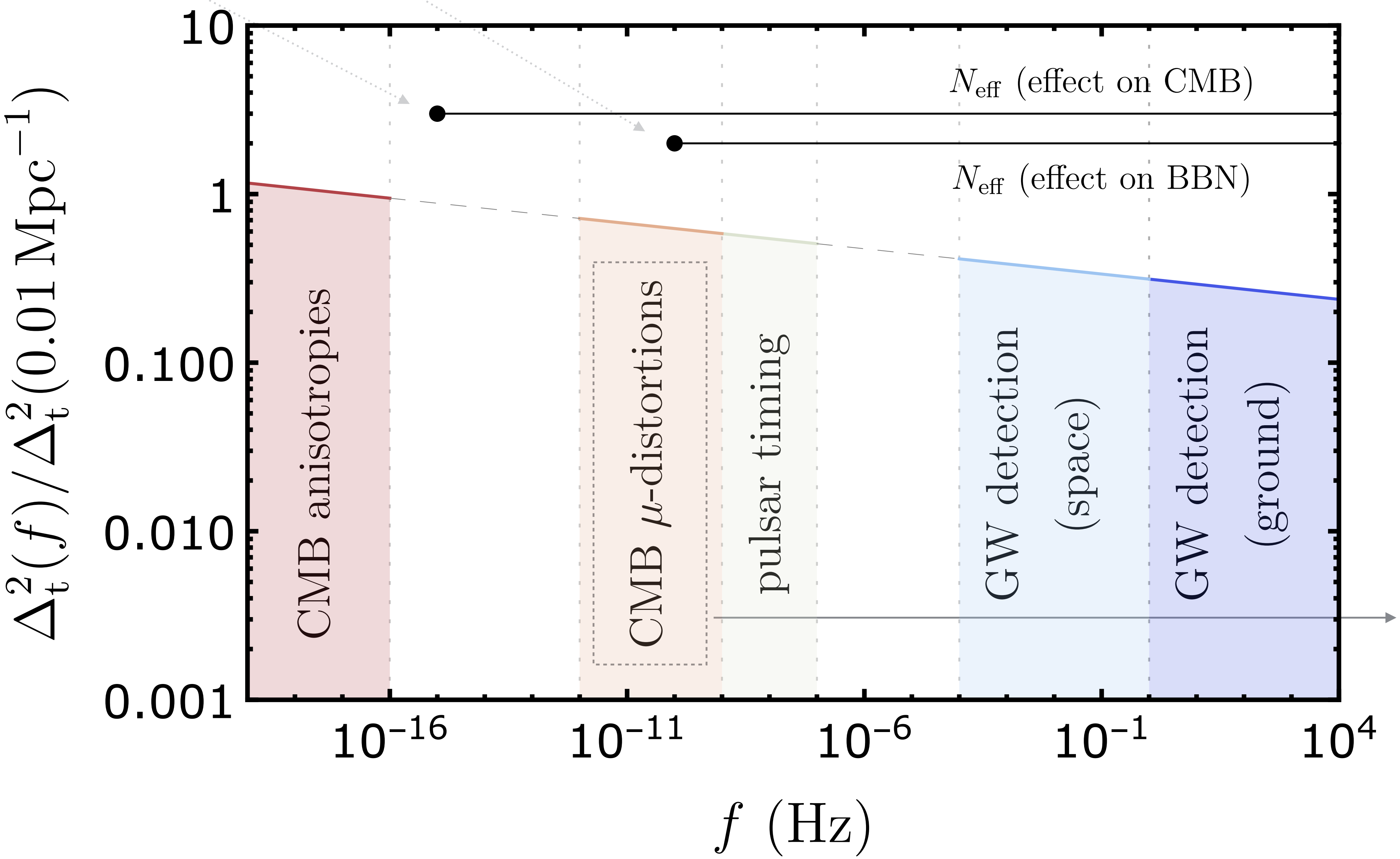

Ota et al., 2014
Chluba et al., 2014

Multi-Wavelength Constraints from Current Data

Constraints from (not so) current data

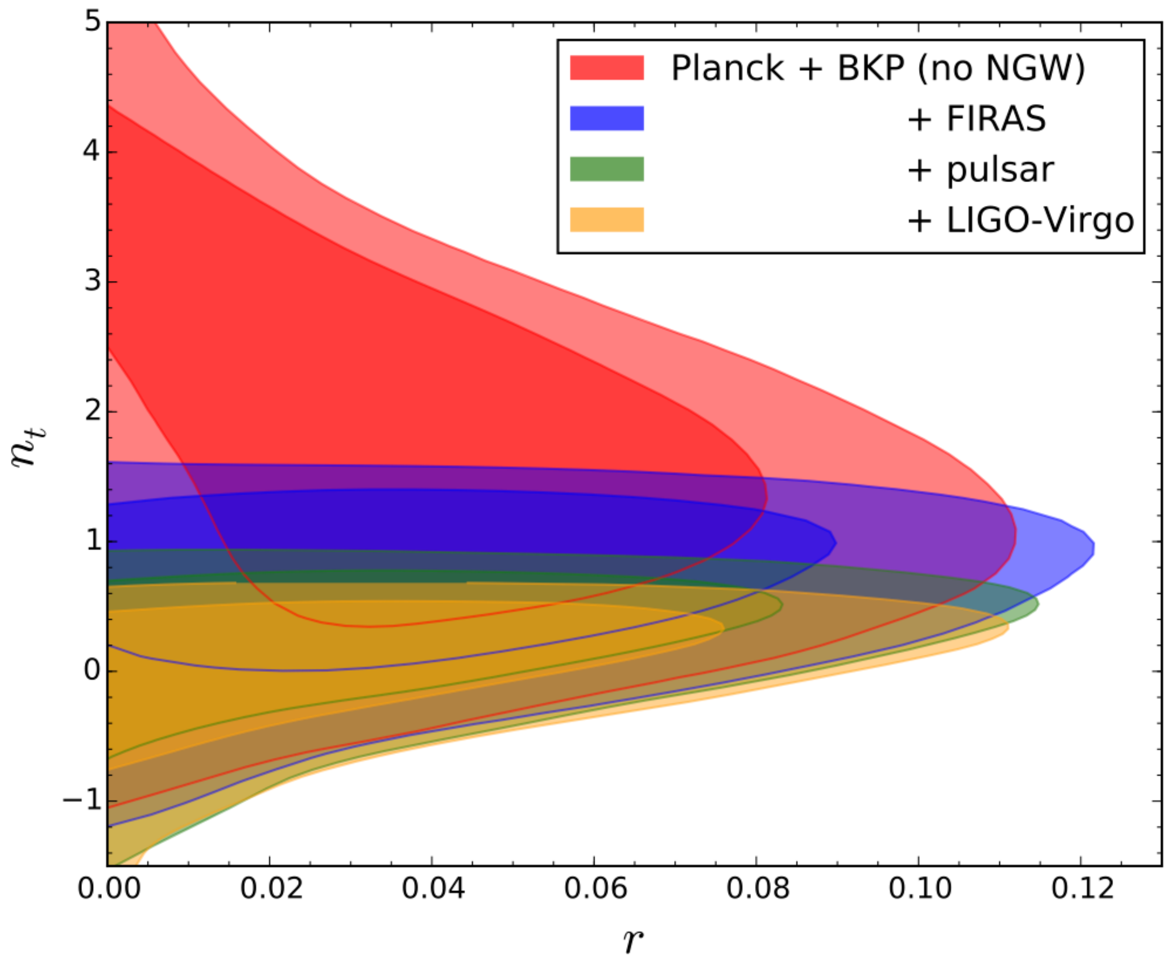

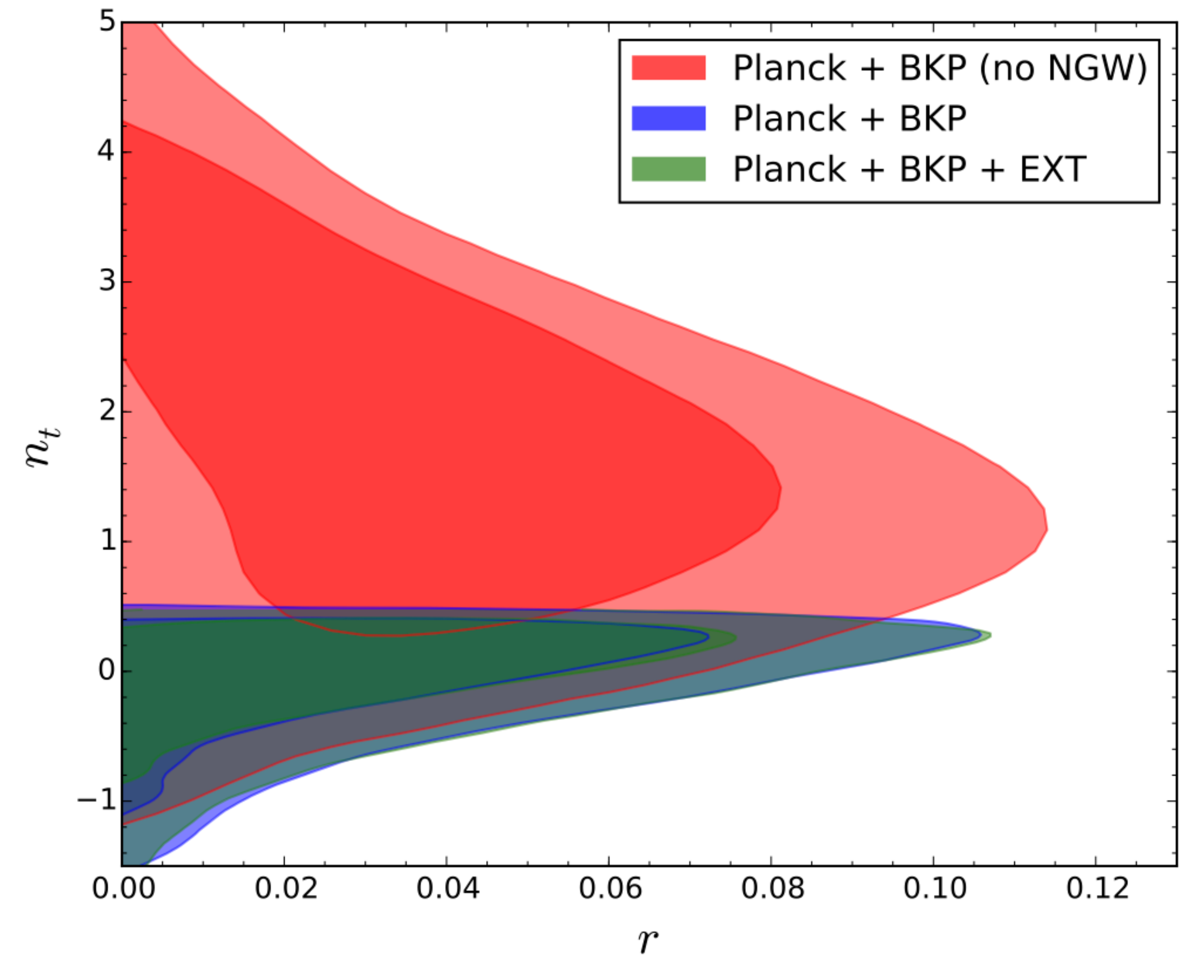

95% CL constraints

Dataset	r	$n_{\rm t}$
Planck + BKP	< 0.089	$1.7^{+2.2}_{-2.0}$
Planck + BKP + FIRAS	< 0.098	$0.65^{+0.86}_{-1.1}$
Planck + BKP + pulsar	< 0.088	$0.20^{+0.69}_{-0.96}$
Planck + BKP + LIGO-Virgo	< 0.085	$0.04^{+0.61}_{-0.85}$
Planck + BKP, with $N_{\rm eff}^{\rm GW}$	< 0.082	$-0.05^{+0.58}_{-0.87}$
Planck + BKP + EXT, with $N_{\rm eff}^{\rm GW}$	< 0.080	$-0.05^{+0.57}_{-0.80}$
Planck + BKP + aLIGO	< 0.078	$-0.09^{+0.54}_{-0.78}$

BAO + Deuterium

- $k_\star = 0.01$: need blue $n_{\rm t}$ for low tensor power at small ℓ;
- additional datasets: cut $n_{\rm t}$ exponentially $\Rightarrow$ r is lowered;
- adding $N_{\rm GW}$: tighter constraints than external datasets.

AdvLIGO: 10× improvement of LIGO

⇩

still no detection from interferometers
but stronger bounds than CMB + $N_{\rm eff}^{\rm GW}$

Constraints from current data

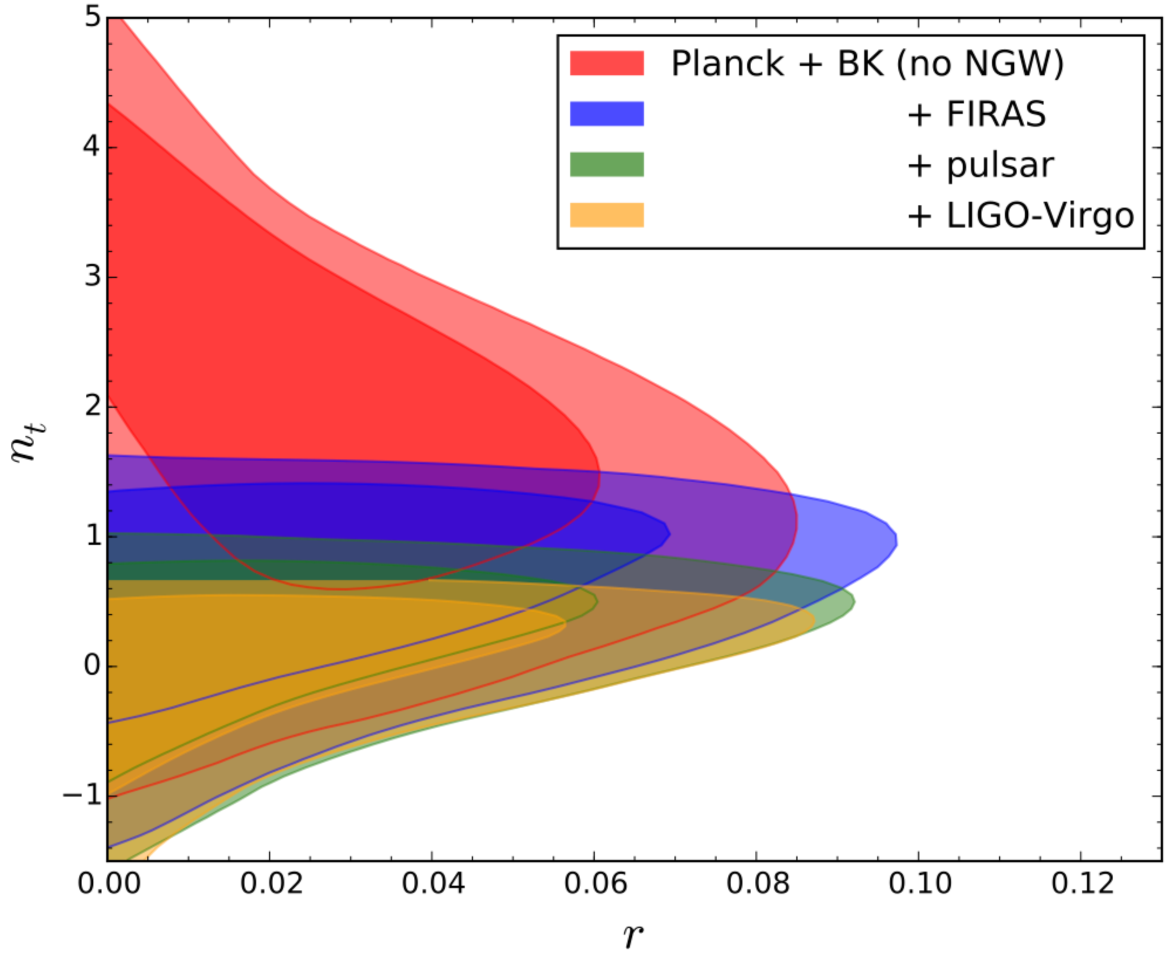

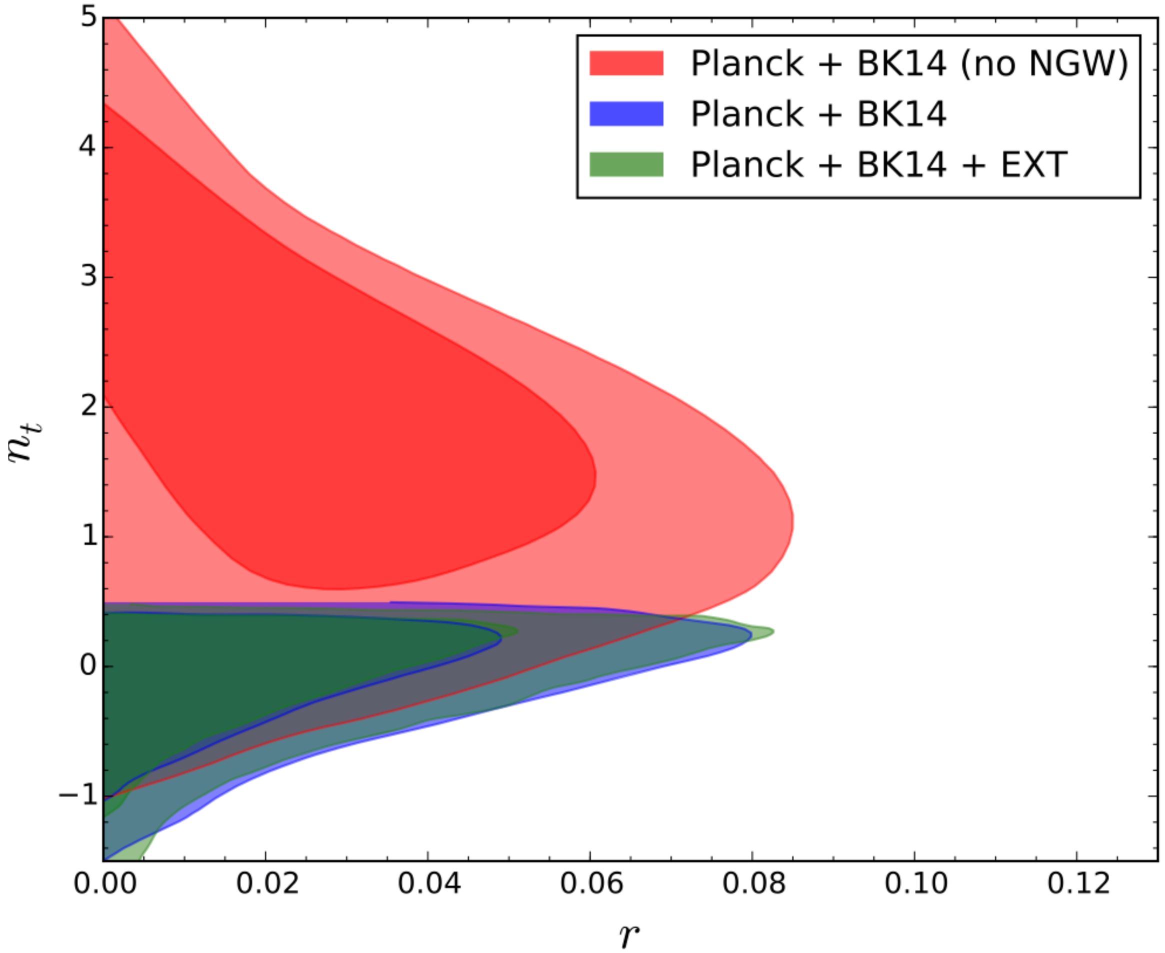

95% CL constraints

Dataset	r	n_t
Planck + BK14	< 0.067	$1.8^{+2.0}_{-2.1}$
Planck + BK14 + LIGO-Virgo	< 0.067	$0.00^{+0.68}_{-0.91}$
Planck + BK14, with $N_{\rm eff}^{\rm GW}$	< 0.061	$-0.12^{+0.65}_{-0.84}$
Planck + BK14 + EXT, with $N_{\rm eff}^{\rm GW}$	< 0.061	$-0.10^{+0.63}_{-0.88}$
Planck + BK14 + aLIGO	< 0.060	$-0.16^{+0.63}_{-0.88}$

smaller error bars from BK14

$\Rightarrow$ tighter constraints on r

however

loss of sensitivity to $n_{\rm t}$

$\Rightarrow$ constraints on $n_{\rm t}$ do not improve a lot

Forecasts:
CMB and Direct Detection Experiments

Forecasts for COrE-like mission

COrE specifics (COrE Collab., 2011)

channel (GHz)	FWHM (arcmin)	$w^{-1/2}$ — T (μK · arcmin)	$w^{-1/2}$ — Q, U (μK · arcmin)
105	10	2.68	4.63
135	7.8	2.63	4.55
165	6.4	2.67	4.61
195	5.4	2.63	4.54
225	4.7	2.64	4.57

additional frequency channels (from 45 GHz to 795 GHz): used for foreground removal

Simulated likelihood (for simplicity consider only B-mode spectra) $\rightarrow$

$$L = \sum_\ell (2\ell+1)\left[-1 + \frac{\hat{C}_\ell^{\mathrm{tens}} + \hat{C}_\ell^{\mathrm{lens}} + N_\ell}{C_\ell^{\mathrm{tens}} + C_\ell^{\mathrm{lens}} + N_\ell} + \log\left(\frac{C_\ell^{\mathrm{tens}} + C_\ell^{\mathrm{lens}} + N_\ell}{\hat{C}_\ell^{\mathrm{tens}} + \hat{C}_\ell^{\mathrm{lens}} + N_\ell}\right)\right]$$

- $\hat{C}_\ell$: evaluated for cosmological parameters that describe the (assumed) true universe
- assuming a Gaussian beam, N_ℓ is

$$N_\ell = \left(\sum_i w_{(i)} e^{-\sigma^2_{(i)}\ell(\ell+1)}\right)^{-1}$$

Delensing

For an experiment with a noise level of order $\sim 1\,\mu\text{K}\cdot\text{arcmin}$ post component separation, one can delens up to 10% (Errard et. al, 2015): COrE can do it.

$$C_\ell^{\text{lens}} \to 0.1 \times C_\ell^{\text{lens}}, \qquad \hat{C}_\ell^{\text{lens}} \to 0.1 \times \hat{C}_\ell^{\text{lens}}$$

Creminelli et al., 2015

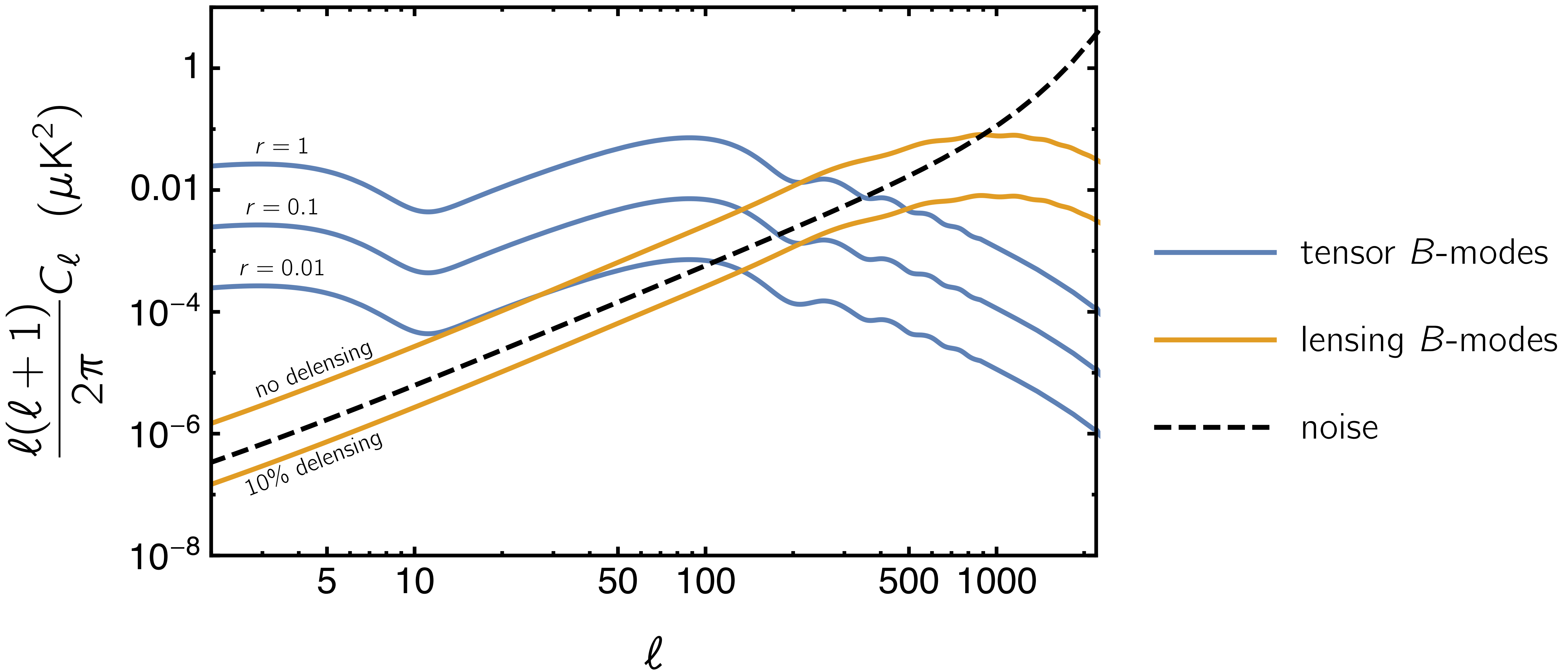

Results of COrE forecasts

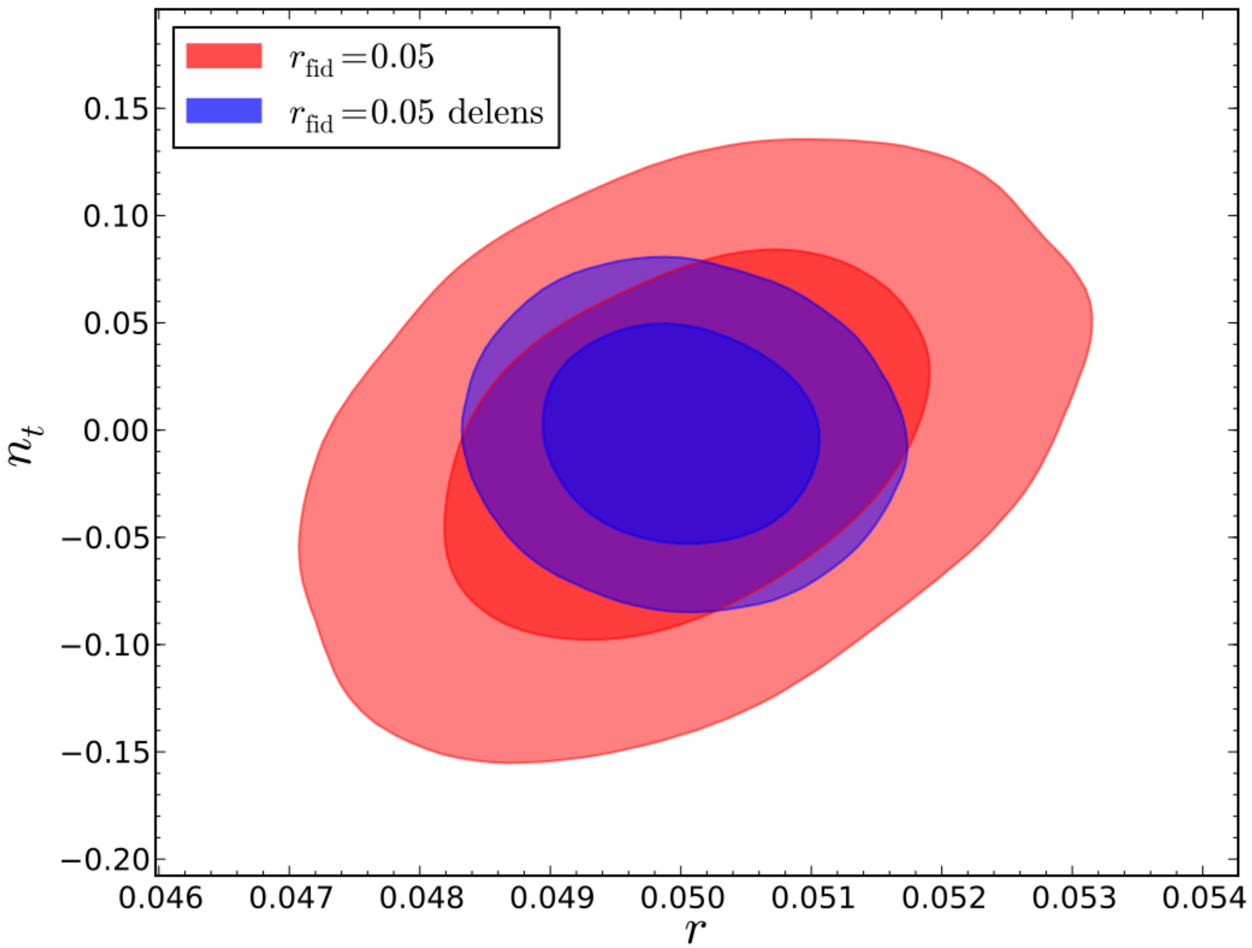

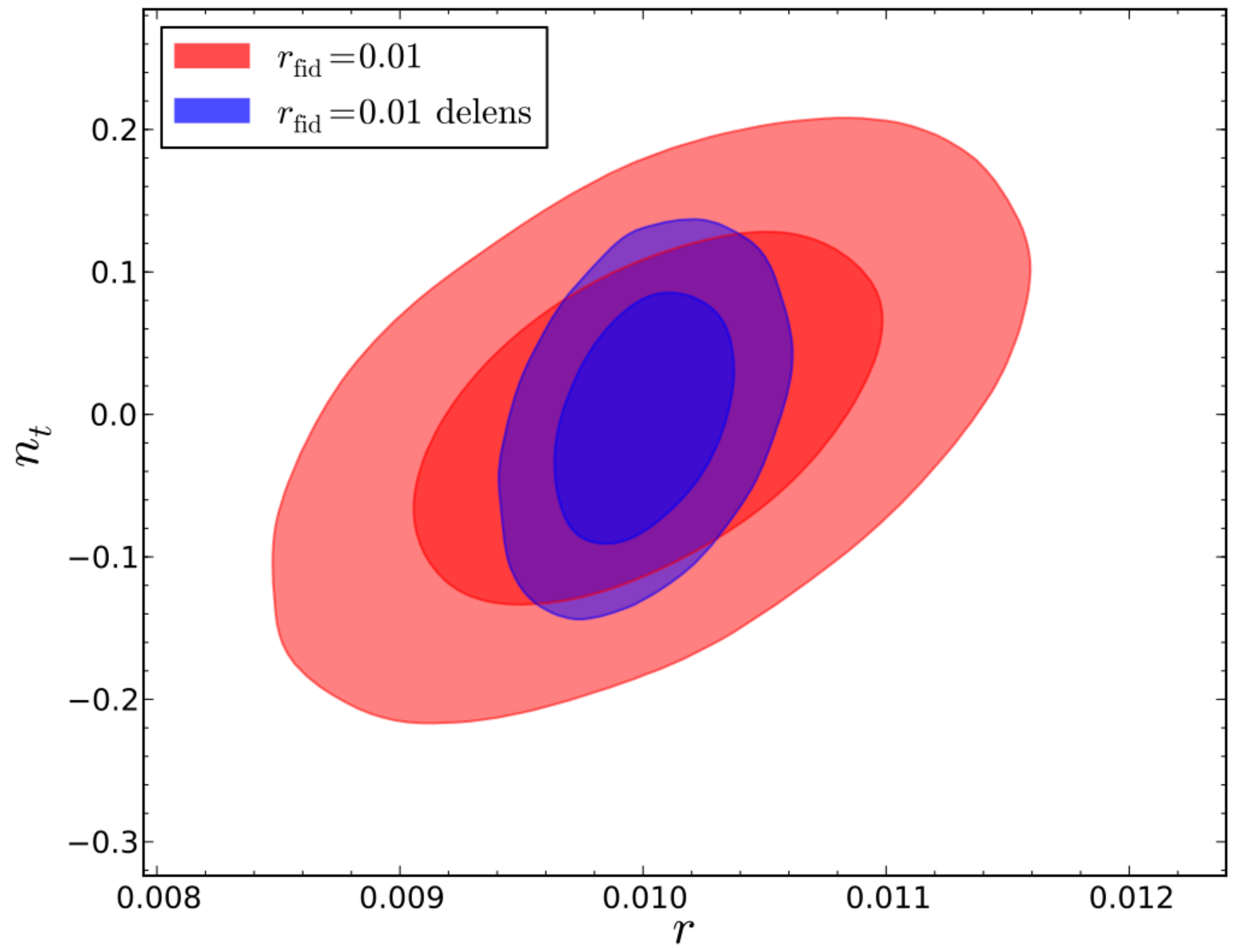

95% CL constraints

	r	$n_{\rm t}$
fiducial	0.05	$-r/8 = -0.00625$
COrE	0.0500 ± 0.0012	$-0.0072^{+0.1108}_{-0.1143}$
COrE, delens.	0.05000 ± 0.00066	$-0.0023^{+0.0632}_{-0.0640}$
fiducial	0.01	$-r/8 = -0.00125$
COrE	0.01001 ± 0.00061	$-0.0024^{+0.1597}_{-0.1637}$
COrE, delens.	0.01000 ± 0.00024	$-0.0019^{+0.1074}_{-0.1088}$

- 10% delensing: break degeneracy between r and $n_{\rm t}$;
- r measured with a relative uncertainty of order 5×10^{-2};
- even with delensing, COrE cannot probe $n_{\rm t} = -r/8$.

COrE + AdvLIGO forecast

	r	n_{t}
fiducial	0.045	0.35
P + BKP + aLIGO	< 0.095	0.354 ± 0.020
COrE	0.0450 ± 0.0011	0.348 ± 0.061
COrE, delens.	0.04500 ± 0.00060	0.350 ± 0.029
COrE + aLIGO	0.0450 ± 0.0010	0.3483 ± 0.0053

AdvLIGO will see Ω_{GW}, but *Planck* will not see r

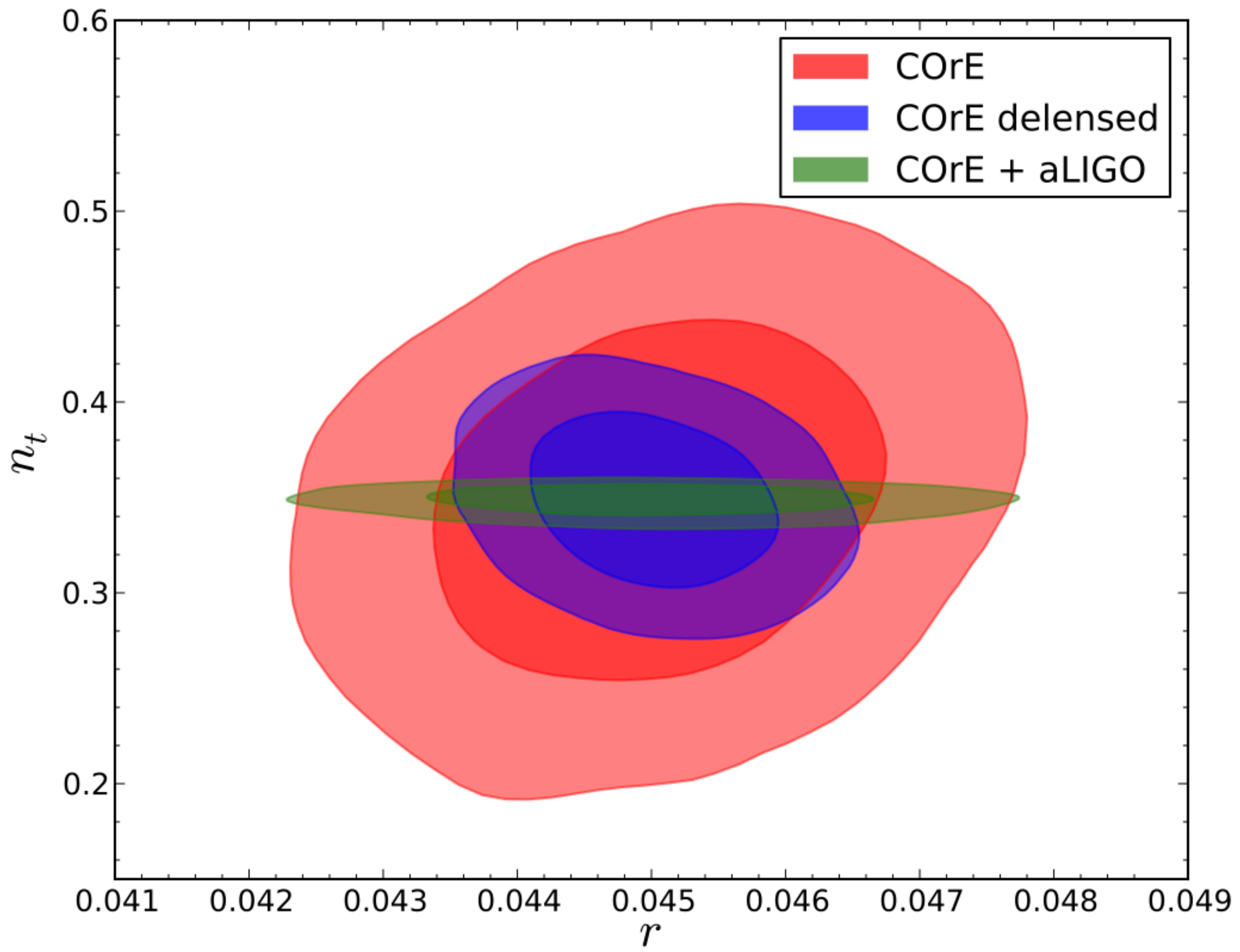

$\sim$ 10x improvement in $\sigma_{n_{\mathrm{t}}}$

important to combine CMB with high-frequency observables

Conclusions

- constraints from small-scale probes forbid very blue $n_{\rm t}$, resulting in tighter bounds on r;
- including contribution of GWs to $N_{\rm eff}$ gives the strongest bounds, comparable to AdvLIGO;
- new BK14 data improve constraints on r, but not on $n_{\rm t}$;
- forecasts for COrE-like mission – 5 channels (assuming that foregrounds are subtracted). Fiducials with $n_{\rm t} = -r/8$:
  - $\sigma_r/r \approx 10^{-2}$;
  - COrE will not be able to test $n_{\rm t} = -r/8$ with high accuracy;
- combining CMB with small-scale probes will be necessary.

Backup slides

Linear sampling and priors on r

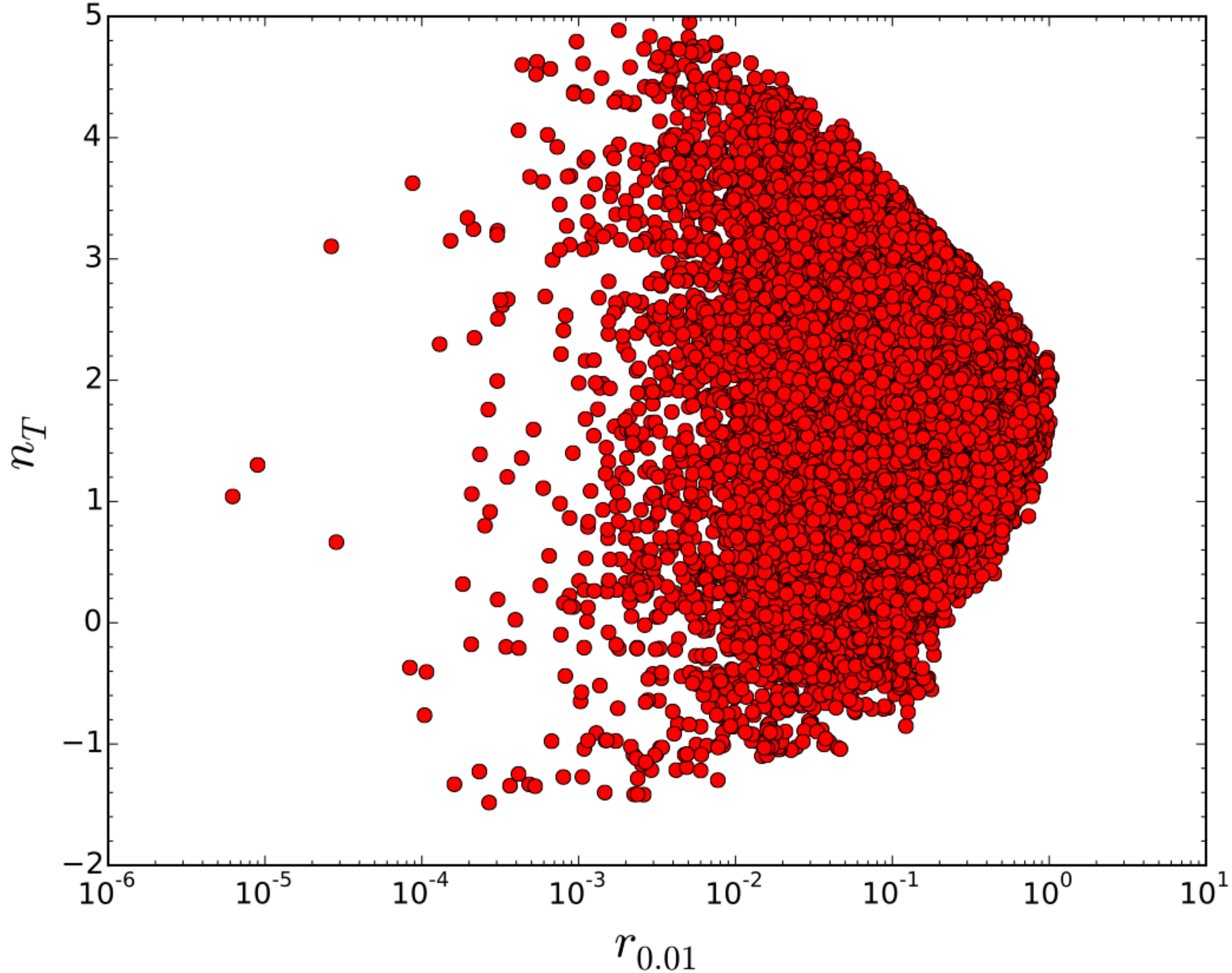

NEC and blue tilt

Consistency relation between $\epsilon_H \equiv -\dot{H}/H^2$ and $n_{\rm t} \rightarrow$

$$n_{\rm t} = -2\epsilon_H$$

EFT for π in decoupling limit (where the mixing between gravity and inflaton is negligible):

$$\mathcal{L}_\pi = -M_{\rm P}^2\dot{H}\underbrace{\left(\dot{\pi}^2 - \frac{(\partial_i\pi)^2}{a^2}\right)} + 2M_2^4\left(\dot{\pi}^2 + \dot{\pi}^3 - \dot{\pi}\frac{(\partial_i\pi)^2}{a^2}\right) + \dots\,,$$

coefficient of $(\partial_i\pi)^2$ is $M_{\rm P}^2\dot{H}$ → $\dot{H}$ must be smaller than zero to avoid instabilities

→ FLRW metric: $\dot{H} < 0$ is the Null Energy Condition, *i.e.* $T_{\mu\nu}k^\mu k^\nu > 0$ for all lightlike k^μ.

Suitable choice of higher derivative operators → can have $\dot{H} > 0$ while maintaining stability (Creminelli et al., 2006).

Number of e-folds of inflation

Number $N_\star$ of e-folds of inflation after $k_\star$ has left the horizon

$$N_\star \equiv \log \frac{a_{\rm end}}{a_\star} = -\log \frac{k_\star}{H_0} + \log \frac{H_\star}{H_0} + \log \frac{a_{\rm end}}{a_{\rm reh}} + \log \frac{a_{\rm reh}}{a_0}$$

where $t_{\rm end}$ marks the transition to radiation dominance.

Standard assumption: reheating is a period of matter domination. Then $\rightarrow$

$$\frac{k_{\rm end}}{\rm Mpc^{-1}} = T_{\rm CMB} \exp\left[\log \sqrt[3]{\beta} - \log\sqrt{3} + \log\sqrt[3]{\alpha^2} + \log\sqrt[3]{\frac{\pi^2}{45} g_*(T_{\rm CMB})}\right]$$

- $E_{\rm end} = (\alpha M_{\rm P})^4$: energy density at the end of inflation;
- $T_{\rm reh} = \beta M_{\rm P}$: temperature at beginning of radiation dominance.

Assuming to have instant reheating ($\alpha = \beta$) at the GUT scale $E_{\rm end} \approx 10^{16}\,{\rm GeV}$

$\Downarrow$

$$k_{\rm end} \approx 2 \times 10^{23}\,{\rm Mpc}^{-1}$$